JOURNAL OF PHARMA INSIGHTS AND RESEARCH ISSN NO. 3048-5428

RESEARCH ARTICLE

Formulation and Characterization of Plumbagin Matrix Tablets Using a Grafted Polysaccharide Carrier for Direct Compressibility and pH-Sensitive Drug Release

Kalyani Sakure*[1], Alok Singh Thakur[2], Madhulika Pradhan[3], Hemant Badwaik[4]

[1] *Department of Pharmaceutics, Rungta College of Pharmaceutical Sciences and Research, Bhilai, Chhattisgarh, India*
[2] *Department of Pharmaceutical Chemistry, Shri Shankaracharya Institute of Pharmaceutical Sciences and Research, Bhilai, Chhattisgarh, India*
[3] *Department of Pharmacy, Rungta International Skills University, Bhilai, Chhattisgarh, India*
[4] *Department of Pharmacy, Shri Shankaracharya Professional University, Bhilai, Chhattisgarh, India*

Publication history: Received on 15th January 2026; Revised on 23rd February 2026; Accepted on 24th February 2026

Article DOI: 10.69613/tpjysd30

Abstract: In this study, directly compressible plumbagin (PLB) matrix tablets were prepared using a modified poly(acrylamide)-grafted-carboxymethyl xanthan gum (CMXG-g-PAAm) polymer. Chemical compatibility between the naphthoquinone bioactive and the polymeric carrier was established via Fourier Transform Infrared Spectroscopy (FTIR), showing no deleterious interactions. Evaluation of the powder blend for pre-compression attributes indicated excellent flowability and packing properties, facilitating efficient processing via the direct compression technique. The resulting tablets complied with all pharmacopeial standards regarding weight uniformity, mechanical strength, and drug loading. Stability studies conducted over a six-month duration under accelerated conditions confirmed the robust nature of the dosage form. Dissolution studies revealed a significant pH-dependent modulation of drug release. In an acidic environment, the formulation exhibited a release profile governed primarily by diffusion coupled with moderate matrix participation. On the other hand, at intestinal pH levels, the system transitioned to near zero-order kinetics. This shift is attributed to the substantial swelling and erosion behavior of the CMXG-g-PAAm matrix in neutral-to-alkaline conditions. These results indicate that the developed matrix system provides an effective platform for the sustained delivery of plumbagin, potentially improving therapeutic outcomes through prolonged residence and controlled absorption within the intestinal tract.

Keywords: Plumbagin; Matrix tablets; Direct compression; CMXG-g-PAAm; Release kinetics.

1. Introduction

Natural bioactive metabolites derived from botanical sources serve as a fundamental reservoir for the development of novel therapeutic interventions against diverse pathological conditions. Among these, Plumbagin (PLB), a primary naphthoquinone constituent found in the roots of *Plumbago zeylanica* L., has garnered significant attention in pharmaceutical research [1]. This plant, indigenous to South Asian regions, is traditionally recognized in various medicinal systems for its broad pharmacological profile [2, 3]. Chemically identified as 5-hydroxy-2-methyl-1,4-naphthoquinone, PLB exhibits a spectrum of biological activities including anti-inflammatory, antioxidant, and anti-rheumatic properties [4-6]. Moreover, its efficacy as an antimicrobial, antimalarial, neuroprotective, and anticancer agent has been documented in various preclinical models [7-13].

The formulation of PLB into effective delivery systems remains a priority to ensure optimal bioavailability and patient compliance although it has great therapeutic potential. Oral solid dosage forms, particularly tablets, remain the most prevalent choice in therapy due to their dose precision, manufacturing economy, and high patient adherence [14]. Among the various tablet manufacturing techniques, direct compression stands out as a highly efficient and cost-effective methodology. This process reduces processing time, minimizes energy consumption, and limits the exposure of sensitive drug molecules to moisture and thermal stress, by bypassing the granulation stage, thereby enhancing the overall stability of the final product [15]. The present investigation is based on the delivery of PLB via various platforms, including self-emulsifying systems and various solubility enhancement methodologies [7, 8, 16]. Additionally, the utility of xanthan gum-based derivatives as suitable carriers for direct compression has been reported [17, 18]. Basing on this literature, the present research focuses on the fabrication and evaluation of PLB matrix tablets utilizing a specialized CMXG-g-PAAm copolymer to achieve sustained release and improved compressibility.

* Corresponding author: Kalyani Sakure

2. Materials and Methods

2.1. Materials

Plumbagin (98% purity) was obtained from P.C. Chem, Mumbai, India. Xanthan gum, acrylamide, and ammonium persulfate were procured from Loba Chemie, Mumbai, India. Analytical grade reagents were used for all experimental procedures without further purification.

2.2. Fabrication of CMXG-g-PAAm Copolymer

The development, purification, and structural characterization of poly(acrylamide)-grafted-carboxymethyl xanthan gum (CMXG-g-PAAm) were performed according to the established protocols previously detailed by our research group [19].

2.3. Preformulation

2.3.1. Chemical Compatibility via FT-IR

The chemical integrity of PLB in the presence of the polymer was evaluated through Fourier Transform Infrared (FTIR) spectroscopy. Spectra for the pure drug, the CMXG-g-PAAm carrier, and the finalized matrix formulation (F1) were obtained using a Shimadzu IRPrestige-21 spectrophotometer. Samples were prepared by the potassium bromide (KBr) pellet technique and scanned within the range of 4000-400 cm^{-1} to identify any shifts or disappearances of characteristic functional group peaks.

2.3.2. Micromeritic Properties

The flow and packing characteristics of the PLB-polymer blend were determined to ensure suitability for direct compression. Parameters including bulk density, tapped density, Carr's compressibility index, Hausner's ratio, and the angle of repose were determined using standardized pharmaceutical methods.

Angle of Repose: The fixed funnel method was utilized to determine the angle of repose (θ). A measured quantity of the powder blend was allowed to flow through a funnel to form a conical heap. The height (h) and radius (r) of the heap were used to calculate the angle using the following equation:

$$\tan \theta = h/r$$

All measurements were performed in triplicate.

Bulk and Tapped Density: A 20 g sample of the blend was placed in a 100 mL graduated cylinder to determine the initial volume (V0) for bulk density calculation. Subsequently, the cylinder was subjected to 100 taps using a tapped density tester (ETD-1020, Electrolab) to record the tapped volume (Vf). Densities were calculated as the ratio of mass to volume.

Compressibility and Hausner's Ratio: The Carr's Index (CI) and Hausner's Ratio (HR) were derived from the density data to quantify the flowability of the blend:

$$CI = [(\text{Tapped Density} - \text{Bulk Density})/\text{Bulk Density}] * 100$$

$$HR = \text{Tapped Density}/\text{Bulk Density}$$

2.4. Preparation of PLB Matrix Tablets

The matrix tablets were prepared by the direct compression of a homogeneous blend consisting of PLB and CMXG-g-PAAm in a 1:1 ratio. Magnesium stearate (1.0% w/w) was incorporated as a lubricant. Compression was performed using a four-station rotary tablet press (Lab press 1, Shakti Pharmatech) fitted with 8 mm biconvex tooling.

2.5. Physical and Chemical Evaluation of Tablets

The tablets were characterized for various quality control parameters. Thickness and diameter were measured for twenty units using a digital vernier caliper. Weight variation was assessed by weighing individual tablets and determining the mean weight. Hardness

was tested using a Monsanto hardness tester (n=6), and friability was evaluated using a Roche friabilator. Drug content uniformity was determined by UV-Visible spectrophotometry at 419 nm after dissolving the crushed tablet powder in pH 6.8 phosphate buffer.

2.6. *In vitro* Dissolution Studies

Release profiles were obtained using a USP Type I (basket) apparatus at 50 rpm in 900 mL of 0.1 N HCl (pH 1.2) and phosphate buffer (pH 6.8). The temperature was maintained at 37 ± 0.5ºC. Samples were withdrawn at specific intervals, filtered, and analyzed spectrophotometrically at 419 nm. Sink conditions were maintained throughout the study.

2.7. Mathematical Modeling of Release Kinetics

To clarify the mechanism of drug transport, the release data were fitted into various mathematical models, including:

- Zero-order ($Qt = Q0 + K0t$)
- First-order ($\ln Qt = \ln Q0 + K_1t$)
- Higuchi model ($Q = KH\ t_{1/2}$)
- Korsmeyer–Peppas model ($Mt/M\infty\} = Kt^n$)
- Hixson–Crowell model ($W_0^{1/3} - W_t^{1/3} = K_st$)

2.8. Accelerated Stability Testing

Stability of the prepared tablets was evaluated according to ICH Q1E guidelines. Tablets were stored in a stability chamber at 40± 2ºC / 75 ± 5% RH and 25 ± 2 ºC / 60 ± 5% RH. Samples were stored and evaluated over six months for any changes in physical appearance, mechanical strength, and dissolution characteristics.

3. Results and Discussion

3.1. Characterization of the CMXG-g-PAAm Carrier

The modification of carboxymethyl xanthan gum via grafting was confirmed through spectroscopic analysis [17, 19]. The FTIR profile showed characteristic absorption bands at 3404.51 cm^{-1} and 3332.01 cm^{-1}, indicating the stretching of hydroxyl and amine groups. The peak at 2891.52 cm^{-1} corresponds to aliphatic C-H stretching. Crucially, the presence of amide I and II bands at 1685.12 cm^{-1} and 1625.42cm^{-1} confirms the integration of acrylamide chains onto the polysaccharide backbone. A characteristic sharp signal at 1732.97 cm^{-1} indicated the presence of carboxyl groups.

3.2. Chemical Compatibility

The FTIR spectrum of pure PLB exhibited sharp peaks at 1649.63 cm^{-1} and 1606.12 cm^{-1}, representing the carbonyl stretching of the naphthoquinone ring. In the matrix formulation (F1), these essential markers were retained without significant shifts, appearing at 1649.63 cm^{-1} and 1605.12 cm^{-1}. The preservation of these functional group signals alongside the polymer-specific peaks indicates the absence of chemical incompatibility, ensuring that the bioactive molecule remains stable within the matrix.

3.3. Micromeritic Properties and Flow Characteristics

The powder blend intended for direct compression was evaluated for flowability, with results summarized in Table 1. The angle of repose was found to be 30.003 ± 0.537º, which classifies the blend as having good flow properties. The Carr's index was 10.880 ± 0.625% and the Hausner's ratio was 1.122 ± 0.007, both indicating excellent compressibility. These favorable micromeritic properties ensure uniform die filling and prevent processing defects like capping or weight variation during high-speed compression.

3.4. Physicochemical Properties of Matrix Tablets

The compressed tablets showed high physical integrity and uniformity. The average weight was 151.535 ± 0.191 mg, with a drug assay value of 98.46 ± 0.609%, confirming precise dose distribution. The hardness was maintained at 5.65 ± 0.09 kg/cm^2, providing sufficient mechanical strength to withstand handling while maintaining low friability 0.525 ± 0.008%. Geometric parameters were consistent, with a thickness of 2.99 ± 0.004 mm and a diameter of 8.085 ± 0.017 mm.

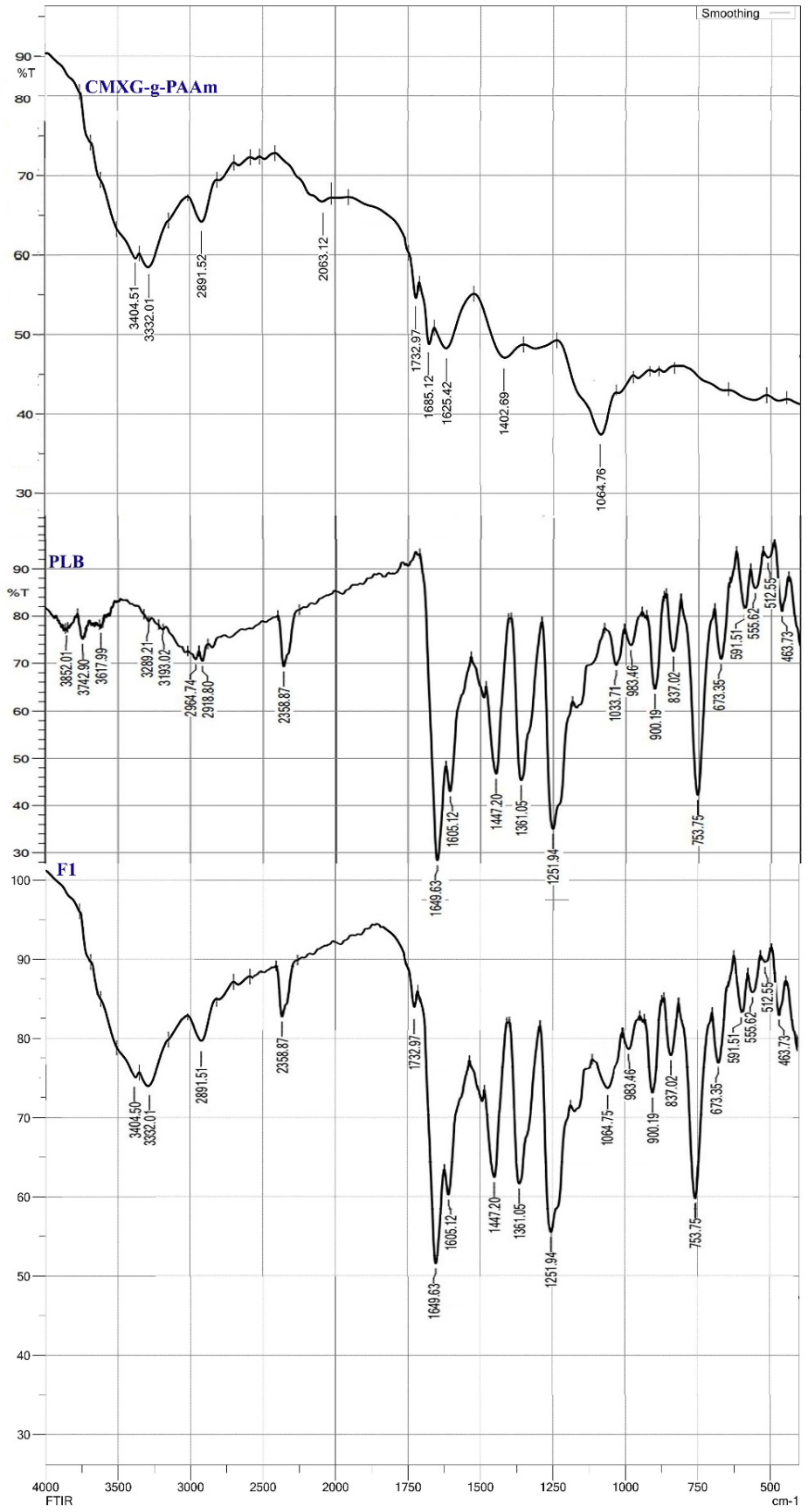

Figure 1. FTIR spectra of PLB, CMXG-g-PAAm, and Formulation F1 (from top to bottom)

Table 1. Pre-compression characteristics of the PLB matrix tablet blend of the prepared Formulation F1

Sl No	Precompression Parameter	Results*
01	Tapped density (g/cc)	0.704± 0.008
02	Bulk density (g/cc)	0.627 ± 0.003
03	Compressibility index (%)	10.880 ± 0.625
04	Hausner index	1.122 ± 0.007
05	Angle of repose (θ)	30.003 ± 0.537

**All values represent mean ± SD; (n = 3)*

Table 2. Characterization of the PLB matrix tablets (F1)

Sl No	Precompression Parameter	Results
01	Thickness (mm)[a]	2.99 ± 0.004
02	Diameter (mm)[a]	8.085 ± 0.017
03	Average weight (mg)[a]	151.535 ± 0.191
04	Hardness (kg/cm²)[b]	5.65 ± 0.09
05	Assay (%)[b]	98.46 ± 0.609
06	Friability (% w/w)[b]	0.525 ± 0.008

**All values represent mean ± SD; (n = 3)*

3.5. Drug Release Kinetics and Mechanisms

The drug release behavior exhibited a distinct sensitivity to the pH of the dissolution medium. In the gastric-simulated environment (0.1 N HCl), 50% of the drug was released in 2.48 h. In the intestinal-simulated medium (pH 6.8), the release was more controlled, reaching 90% at 5.49 h (Table 3).

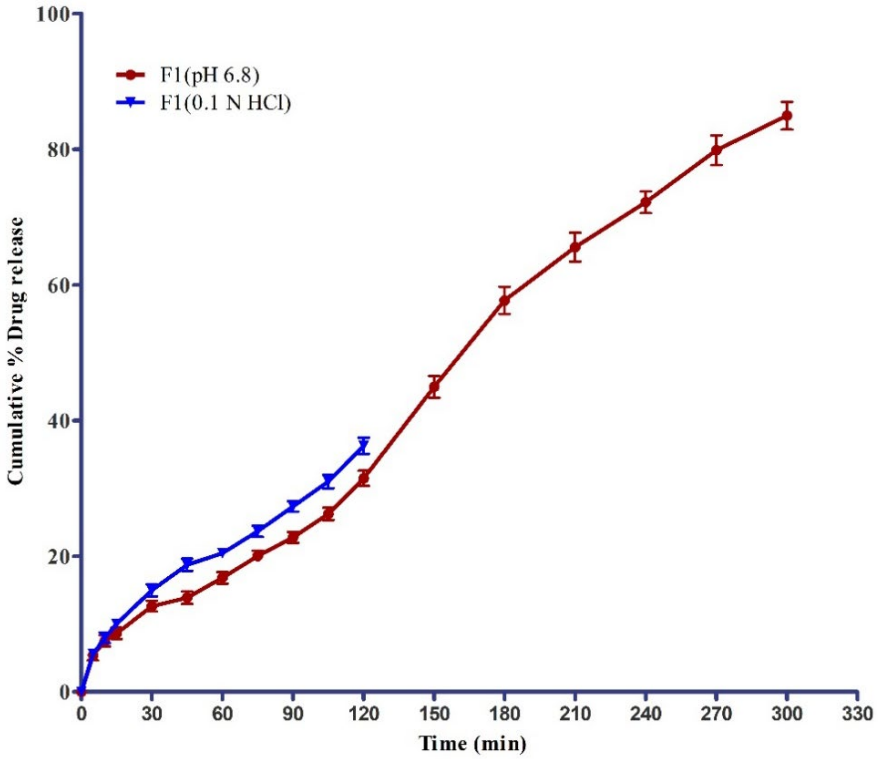

Figure 2. *In vitro* release of PLB from formulation F1 in pH 1.2 and pH 6.8 media

Table 3. Cumulative percentage release data of PLB from formulation F1

Formulation code	Time (h)	CDR 1	CDR 2	CDR 3	Mean	SD	$T_{50\%}$
F1 in 0.1 N HCl	0	0.00	0.00	0.00	0	0	2.48
	0.25	9.48	10.02	10.63	10.04	0.575	
	0.5	14.12	15.88	14.91	14.97	0.881	
	0.75	18.02	18.41	19.74	18.72	0.901	
	1	19.84	20.49	21.02	20.45	0.591	
	1.25	23.95	22.75	24.31	23.67	0.816	
	1.5	26.48	27.55	27.99	27.34	0.776	
	1.75	32.02	31.04	30.01	31.02	1.005	
	2	36.16	37.53	35.15	36.28	1.194	
Formulation code	**Time (h)**	**CPR 1**	**CPR 2**	**CPR 3**	**Mean**	**SD**	$t_{90\%}$
F1 in pH 6.8	0	0.00	0.00	0.00	0	0	5.49
	0.25	7.81	8.62	9.46	8.63	0.825	
	0.5	11.83	12.65	13.44	12.64	0.805	
	0.75	13.01	13.84	14.82	13.89	0.906	
	1	16.04	16.69	17.74	16.82	0.857	
	1.25	19.28	20.060	20.78	20.04	0.750	
	1.5	21.98	22.78	23.58	22.78	0.800	
	1.75	25.43	26.04	27.23	26.23	0.915	
	2	30.58	31.150	32.74	31.49	1.119	
	2.5	43.40	44.95	46.62	44.99	1.610	
	3	55.69	57.79	59.71	57.73	2.010	
	3.5	63.98	64.79	68.01	65.59	2.131	
	4	70.69	72.02	73.89	72.20	1.607	
	4.5	77.64	79.98	82.03	79.88	2.196	
	5	82.97	84.89	87.05	84.97	2.041	

CDR: Cumulative Drug Release

Kinetic modeling (Table 4) provided more information about the transport mechanism. In acidic conditions, the data best fit the Korsmeyer–Peppas model ($R^2 = 0.9839$) with a diffusional exponent (n) of 0.5854. This value indicates an anomalous (non-Fickian) transport, where drug release is mediated by both diffusion and polymer relaxation. However, at pH 6.8, the system followed zero-order kinetics ($R^2 = 0.9874$). The n value increased to 0.8392, approaching Case II transport. This shift suggests that in intestinal conditions, the expansion and erosion of the grafted polymer matrix become the dominant factors controlling the release rate, providing a constant delivery profile.

Table 4. Statistical parameters for various drug release kinetic models

Formulation code	Higuchi		Hixson-crowell		Koresmeyer–Peppas		Zero order		1st order	
	n	R^2	n	R^2	n	R^2	n	R^2	n	R^2
F1(0.1 N HCl)	24.31	0.974	0.285	0.971	0.585	0.983	15.85	0.961	0.086	0.974
F1 (pH 6.8 buffer)	41.98	0.901	0.435	0.972	0.839	0.949	17.556	0.987	0.16	0.949

3.6. Stability and Shelf-life Evaluation

The matrix formulation remained stable throughout the six-month accelerated study. No significant variations were observed in drug content, weight, or mechanical strength (Table 5). Dissolution profiles after storage were nearly identical to the initial profiles (Figure 3), confirming the robustness of the CMXG-g-PAAm carrier in protecting the PLB molecule from environmental degradation.

Table 5. Results of Stability Studies for PLB matrix tablets over 6 months

Evaluation parameters	Observation in Months						
	Initial	25 ± 2 °C/60 ± 5% RH			40 ± 2 °C/75 ± 5% RH		
		1	3	6	1	3	6
Physical appearance	Matrix Tablet	No change	No change	No change	No change	No change	No change
Average weight (mg)[a]	151.53 ± 0.19	151.75 ±0.16	152.86 ± 0.24	154.13 ± 0.36	151.68 ± 0.23	153.34 ± 0.21	155.67 ± 0.42
Friability (%)[b]	0.52 ± 0.008	0.51 ± 0.21	0.52 ± 0.36	0.54 ± 0.29	0.53 ± 0.23	0.541 ± 0.45	0.55 ± 0.29
Hardness (kg/cm^2)[b]	5.65 ± 0.09	5.55 ± 0.44	5.42 ± 0.51	5.58 ± 0.28	5.42 ± 0.49	5.38 ± 0.42	5.31 ± 0.25
Drug content (%)[b]	98.46 ± 0.609	98.13 ± 0.41	98.05 ± 0.24	97.91± 0.341	98.39 ± 0.23	98.24 ± 0.18	97.82 ± 0.28

[a] Values are mean ± SD (n = 20), [b] Values are mean ± SD (n = 6)

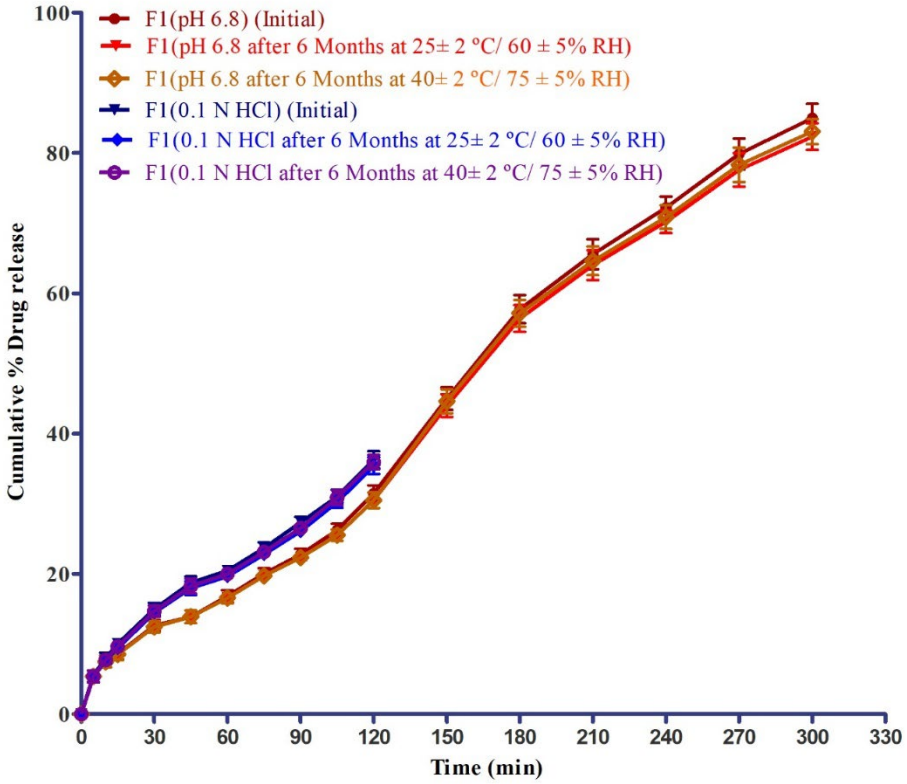

Figure 3. Comparison of drug release of PLB matrix tablets after stability storage

4. Conclusion

The successful preparation of directly compressible plumbagin matrix tablets was achieved utilizing a poly(acrylamide)-grafted-carboxymethyl xanthan gum carrier. Experimental findings confirmed that the powder blend possesses the necessary flow and compression characteristics for efficient industrial-scale processing. The resulting dosage form showed excellent physical stability and chemical compatibility. An important finding is the pH-responsive nature of the delivery system; the matrix provides a sustained, zero-order release profile in intestinal conditions while maintaining integrity in acidic environments. This delivery pattern is pharmacologically advantageous for maximizing the therapeutic efficacy of plumbagin through prolonged intestinal exposure. The study proved that CMXG-g-PAAm is a versatile and robust excipient for the development of sustained-release herbal bioactive formulations.

References

[1] Verma A, Goyal A. Unravelling the potent anti-oxidant and anti-inflammatory actions of plumbagin: A review of preclinical discoveries. *Pharmacol Res - Mod Chin Med.* 2024;10:100351.

[2] Sharma N, Kaushik P. Medicinal, biological and pharmacological aspects of *Plumbago zeylanica* (Linn.). *J Pharmacogn Phytochem.* 2014;3(4):117-120.

[3] Girija S. Effect of sample extraction, preparation methods on HPLC quantification of plumbagin in *in vivo* and *in vitro* plant parts of *Plumbago zeylanica* L. *Afr J Biotechnol.* 2018;17(47):1478-1483.

[4] Galal AM, Raman V, Avula B, Wang YH, Rumalla CS, Weerasooriya AD, et al. Comparative study of three *Plumbago* L. species (Plumbaginaceae) by microscopy, UPLC-UV and HPTLC. *J Nat Med.* 2013;67(3):554-561.

[5] Padhye S, Dandawate P, Yusufi M, Ahmad A, Sarkar FH. Perspectives on medicinal properties of plumbagin and its analogs. *Med Res Rev.* 2012;32(6):1131-1158.

[6] Mukherjee S, Hossain MA, Raj A, Sikdar B, Roy S. The antibacterial and antioxidant activities of plumbagin-rich methanolic root extracts from *Plumbago zeylanica* L. *The Microbe.* 2025;7:100293.

[7] Gupta S, Kesarla R, Omri A. Formulation strategies to improve the bioavailability of poorly absorbed drugs with special emphasis on self-emulsifying systems. *ISRN Pharm.* 2013;2013:848043.

[8] Panigrahi KC, Patra CN, Jena GK, Ghanooni M, Patro CP, Sahu ME, et al. Gelucire-based liquid self-microemulsifying drug delivery system of plumbagin: Design, optimization, and *ex vivo* permeation studies. *ACS Omega.* 2022;7(47):42781-42793.

[9] Zhang X, Chen Y, Chen T, Li B, Tian S. Plumbagin controls fungal postharvest pathogens by affecting metabolism and inducing autophagy. *Postharvest Biol Technol.* 2024;212:112904.

[10] Sumsakul W, Plengsuriyakarn T, Chaijaroenkul W, Viyanant V, Karbwang J, Na-Bangchang K. Antimalarial activity of plumbagin *in vitro* and in animal models. *BMC Complement Altern Med.* 2014;14(1):15.

[11] Khosla G, Sharma V, Shukla VK. Bioactive molecule-based nano-particulate drug delivery system for antifertility activity. *J Dispers Sci Technol.* 2025;46(11):1723-1736.

[12] Ahsan R, Khan S, Khan MM, Mishra A, Ahmad U, Akhtar W. Comparative neuroprotective effects of Phloridzin, Plumbagin, and Berberine chloride in a scopolamine-induced Alzheimer's disease rat model. *Food Biosci.* 2025;106764.

[13] Nazeem S, Azmi AS, Hanif S, Ahmad A, Mohammad RM, Hadi SM, et al. Plumbagin induces cell death through a copper-redox cycle mechanism in human cancer cells. *Mutagenesis.* 2009;24(5):413-418.

[14] Aulton ME, Taylor K. *Aulton's Pharmaceutics: The Design and Manufacture of Medicines.* 5th ed. Elsevier; 2018.

[15] Lieberman HA, Lachman L, Schwartz JB. *Pharmaceutical Dosage Forms: Tablets, Volume 1.* 2nd ed. Marcel Dekker; 1990.

[16] Patel H, Pandey S. Solubility and dissolution rate enhancement of plumbagin using various techniques. *Int J Pharm Sci Rev Res.* 2015;30(1):241-246.

[17] Ahuja M, Kumar A, Singh K. Synthesis, characterization and evaluation of carboxymethyl xanthan gum for sustained release of diltiazem HCl. *Int J Biol Macromol.* 2011;49(4):530-536.

[18] Makhado E, Pandey S, Modibane KD, Kang M, Hato MJ. Synthesis and characterization of xanthan gum-g-poly(acrylamide) for drug delivery applications. *Cellul Chem Technol.* 2019;53(3-4):235-245.

[19] Badwaik HR, Sakure K, Alexander A, Dhongade H, Tripathi DK. Synthesis and characterisation of poly (acryalamide) grafted carboxymethyl xanthan gum copolymer. *Int J Biol Macromol.* 2016;85:361-369